Usage of 3D Printed Polylactic Acid as a Core Material in Forming of Carbon Fiber Fabric Composite

Onur Kaya[1] 0000-0002-8010-6707
Omer Yunus GUMUS[2] 0000-0002-3361-6528
Israfil KUCUK[3] 0000-0002-1284-8880
Serdar ASLAN[4] 0000-0001-5061-6338

[1] Ermetal Automotive / DOSAB, Bursa, Turkiye
[2] Bursa Technical University / Faculty of Engineering and Natural Sciences / Department of Polymer Materials Engineering / Bursa, Turkiye
[3] Gebze Technical University / Institute of Nanotechnology / Kocaeli, Turkiye
[4] Sakarya University / Faculty of Engineering / Department of Metallurgical and Materials Engineering / Sakarya, Turkiye

ABSTRACT

In this study, it is aimed to utilize advantages of additive manufacturing in preparation of laminated composite materials with no need of mold. To do so, the composite was prepared by applying carbon fiber fabric on a polylactic acid (PLA) core produced by additive manufacturing. 2 and 3-laminated samples were used for weight drop tests by applying 50 J of impact energy. Complete damage was observed with 2-laminated samples, while partial damage occurred on 3-laminated samples with 23.63 J absorbed energy. Moreover, the force-time plot showed a characteristic pattern of the composite structure. Tensile tests revealed that the samples exhibited brittle fracture with limited elongation and had no contribution of the PLA core to the stress-strain behavior. However, two stages were observed in the stress-strain curve of three-point bending test which were attributed to the thermoset carbon fiber laminate layer and thermoplastic PLA core. A maximum bending stress was determined as 138.81 MPa.

1. INTRODUCTION

Additive manufacturing refers to technologies in which 3D objects are produced by adding material on top of each other. Among other additive manufacturing techniques, material extrusion, which is also known as fused deposition modeling (FDM), is mostly used one because of its easy-to-use, wide variety of raw materials and low investment cost. Additive manufacturing technologies have attracted great interest in many sectors such as aviation, architecture and medicine, as well as defense, art and education [1]. These technologies help to manufacture lightweight parts with complex geometry, either as prototypes or functional ones [2]. Additive manufacturing technologies have very important advantages such as shortening the design-production cycle, reducing production costs and increasing competitiveness compared to traditional methods in which molds or adjustment required machines are used [3]. Among the additive manufacturing methods, FDM attracts increasing attention due to its low cost, low material loss and ease of use [4].

FDM method is based on solidification of polymer melts deposited layer-by-layer on a surface. However, the weak adhereance between the layers causes easy separation of the layers resulting in poor mechanical properties and damage at an early stage. In addition, the parts produced by the FDM method generally show lower elastic properties than the parts produced by injection molding with the same thermoplastic [5]. Although engineering thermoplastics

such as PEEK or PEI provide a partial improvement in the mechanical properties of the part, the use of these materials in the FDM method has been limited to prototyping. The advantages of the FDM method, such as shortening the design-production cycle, reducing production costs and increasing competitiveness, have increased the interest in using this technology to produce structural parts beyond prototyping in recent years. Various studies have been carried out to produce high-performance composite materials by reinforcing the thermoplastic matrix with particles, fibers or nanomaterials to produce structural parts. [3,6,7]. In the FDM method, there are two methods for producing the part with fiber reinforcement. In the first method, the filament, which is the raw material of the FDM method, is used as pre-reinforced. In the second method, the fiber is directly reinforced during the 3D Printing process.

The strength of the parts produced by the FDM method is directly affected by the bond strength between the layers. Caminero et al. [8] evaluated the interlayer bonding performance of continuous fiber reinforced thermoplastic composite produced with FDM in their study to examine the effect of bond strength between layers. In this study, short-beam shear test was performed on Nylon composites produced with continuous glass, carbon and Kevlar fibers in accordance with ISO standards to determine the shear strength between layers. As a result of this study, it was determined that the interlayer bond strength of nylon samples under unreinforced conditions was directly affected by the layer thickness. While the carbon fiber reinforced composite showed the best interlayer shear performance, Kevlar showed the lowest interlayer shear performance due to the weak interlayer adherence between nylon-kevlar. The production of fiber-reinforced materials with FDM has a great advantage as it does not require molds. However, the mechanical properties of such materials are considerably lower than the composites produced by traditional methods, since the interlayer shearing performance is low. In order to improve the interlayer bond strength of continuous reinforced composites produced with FDM, a compression step is needed in which the porosity can be reduced after filament deposition [8]. Studies show that continuous fiber reinforcement has a significant effect on increasing the strength of the part produced with FDM. Carbon fiber reinforcement ensures that only each layer is strengthened separately. The effect of carbon fiber reinforcement on improving interlayer bond performance is limited.

Sandwich structure model is one of the most common application for supporting a part produced by FDM method with composite structure. Composite sandwich structures are used especially where lightness and strenght are desired. The main load-bearing elements of sandwich structures are the lower and upper panels. Although the main function of the core is to hold the upper and lower panels together, the

geometry of the core directly affects the strength and especially the energy absorption. The production of core of sandwich structures with 3D printing provides flexibility in core geometry. Studies on core of sandwich composites produced with 3D printing show how different geometries effect sandwich panel strength. In their study [9], Li and Wang produced the core of the sandwich-structured composite in different geometries (grid, honeycomb and indented) with a 3D printer and bonded the face sheets to both sides of the core. According to the results of the bending performance of the sandwich structures, it was observed that the highest bending strength was achieved by producing the core in the grid structure. Servestani et al., measured the energy absorption of sandwich-structured samples with the low-velocity impact test. Samples consisting of face plate and core were produced in one piece from PLA material without reinforcement by FDM method. According to the measurement results, the sample with the rectangular core had the highest strength and the sample with the honeycomb core had the highest energy absorption. Li and Wang fabricated the faceplates and 3D-Printed cores singly and bonded them with epoxy adhesive [9]. Bending test results applied to the test specimens provided the highest strength grid structure and showed similarities with the study of Servestani et al. [10]. Lu et al. [11] adhered a carbon fiber epoxy face plate to the cores with different core geometries (Bi-Grid, Tri-Grid, Quadri-Grid and Kagome-Grid) produced with PLA and examined the strength and damage mechanisms of the samples with the three-point bending test. The Quadri-Grid sandwich structure provided the highest bending strength. Studies show that core geometry has a significant effect on part strength.

Studies show that the core produced by 3D printing is compatible with the composite layer bonded to both sides. However, 3D Printed core with face sheets are possible for just flat panel and parts with limited geometry. Kazmi et al. [12] used resin transfer molding (VARTM) method with FDM mold to produce curved composite part. In their study, the FDM mold was separated from the part after the composite process. In their study, Dippenaar and Schreve [13] evaluated the feasibility of infusion molds produced with FDM for the production of composite parts. They researched, the economic life, surface quality and cost of the FDM molds and dimensional tolerances and surface quality of the produced parts. The part produced with the FDM mold has a precision of ±1mm. With the processes such as sanding and painting applied to the molds, a surface finish close to the CNC machined surface quality (2 μm) has been achieved without any significant loss of precision. Mold life is limited to the production of 15 to 30 parts.

Mishra et al. [14] obtained an electromagnetic shield by coating epoxy carbon fiber with vacuum infusion method on a macroporous core produced by FDM method. In their study, the part produced by the FDM method is placed in a

carbon fiber mat, and after the part is removed from the mold and fully cured, when the core is dissolved by immersing it in a solution, pores are formed in the composite structure. This study was carried out to examine the electromagnetic shielding efficiency of the manufactured part, thanks to the metallic particles added into the composite. Besic et al., [15] produced Charpy impact test and three-point bending test specimens by applying only resin to the porous core produced by FDM method with vacuum infusion method without reinforcement material. The samples obtained by this method were compared with the samples made of PLA and their benefits were evaluated. They reported that production of PLA-epoxy composite did not provide significant benefits due to the complexity of producing porous composite parts, and adding epoxy only provided improvements.

As it is understood from the literature review above, 3D-printed parts have been generally used as an external mold to produce composite structures. Some others have used those parts as a component of the sandwich type composites. However, to the best of our knowledge, evaluation of the printed part as a core in laminated fabric composites to give 3D form has not been considered so far. In this study, 3D-printed PLA parts were used to form carbon fiber fabric laminated composites. Dimensional accuracy and weight changes during the process were measured. Effect of core structure and layer number of the fabrics on drop weight impact absorbance were investigated. It is concluded that, besides laminated layers, core structure also has a role in impact absorption. It was determined that core structure does not contribute the tensile properties, while it has a contribution to three-point bending results. It is concluded that 3D-printed parts can be used for 3D forming of carbon fiber fabric composite with no need of a mold. Thus, this technique is offered in a time and cost-effective way to produce robust composite structures with complex designs.

2. MATERIAL AND METHOD

2.1 Material

For the core material, PLA filament having diameter of 1.75 mm and Shore D value of 90 (eSUN Industrial Co., Ltd., Chinia) was used. Twill carbon fiber fabric was purchased from Dost Kimya (Turkiye). Carbon fiber fabric with a weight of 200 gr/m^2 is woven in twill form using T300 HT 3k 200tex as weft fiber and T300 HT 3k 200tex as warp fiber. A spray adhesive (3M, Super 77, USA) was used to fix the fabric on the core. For the preparation of the composites, an epoxy resin (EPIKOTE™ Resin MGS™ RIMR 135, Hexion, USA) and hardener (EPIKURE™ Curing Agents MGS RIMH 137, Hexion, USA) were used.

2.2 Methods

2.2.1 3D Printing of the Cores

The cores of the composite specimens for tensile, three-point bending and drop weight impact tests were printed using an EKSER Plus 3D printer (BenMaker 3D, Tukey) and the printing parameters have been given in Table 1. The faces of the cores are positioned in the X-Y plane on the 3D printer print bed. The geometric dimensions of the produced cores are shared in Figure 1.
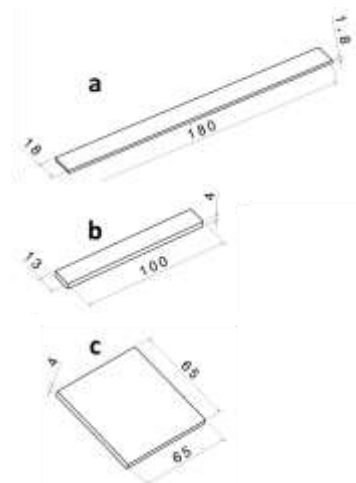

Figure 1. Core dimensions of test specimens in mm a) tensile test specimen, b) three-point bending test specimen and c) drop weight impact test specimen.

2.2.2 Preparetion of the Composites

A tpical preparation of the composites was carried out as follows: The carbon fiber fabric was wrapped over the cores and then the adhesive was sprayed in order to fix the shape until vacuuming. Afterwards, the resin and the hardener, premixed at 70:30 ratios, were applied to the fabrics with the help of a brush. The curing of the resin-impregnated samples was carried out by vacuum bagging method. To do so, the resin-impregnated test specimens were placed in a vacuum bag sealed with a sealent tape as seen in Figure 2. By applying a vacuum pressure of -0.5 bar with a vacuum pump (BUCHI - V-700, Switzerland), hence excess resin was removed from the test samples in the vacuum bag. The test specimens were cured at room temperature under vacuum pressure for 12 hours.

Table 1. 3D Printing parameters of the cores.

Parameter	Value
Layer height	0.2 mm
Shell thickness	0.6 mm
Top/Bottom shell thickness	1.2 mm
Infill pattern	Lines
Infill density	75 %
Print temperature	230 °C
Bed temperature	60 °C
Print Speed	30 mm/s

After each stage, weight of the core, the fabric, and whole sample after curing were determined using a electroninc balance (OHAUS DV215CD, USA) with precision scales. The values are given in Table 2.
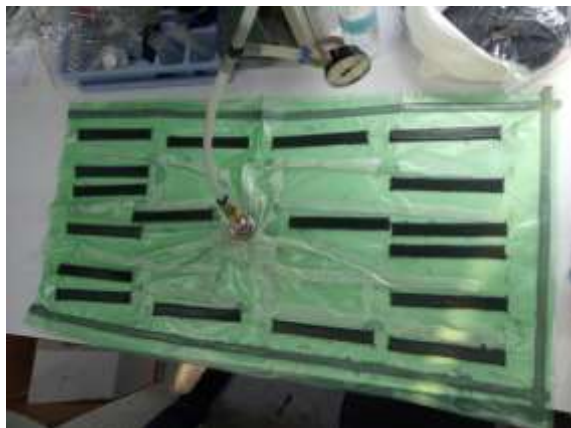

Figure 2. Test specimens placed in vacuum bag.

2.2.3 Drop weight impact

Drop weight impact tests were carried out with the INSTRON - CEAST 9350 free fall mechanical tester. The test specimens are fixed to the holding apparatus located at the bottom of the test device as seen in Figure 3. An additional load of 5 kg is placed on a spherical tip with a diameter of 20 mm on which an impact load is applied. The impact energy is set to 50 J from the user interface of the tester. The free fall mechanical tester releases the load from a height appropriate to the set energy.

Maximum force, time to reach maximum force and impact energy were obtained from the data of drop weight impact test. The absorbed energy is obtained by calculating the difference between the peak impact energy and the impact energy at the zero load.

The spherical tip of the drop weight impact tester penetrated deeply with significant damage to the 2-laminated samples. When the samples are penetrated with complete damage, spherical tip can't transfer its energy fully to the test sample. So, it was decided to increase fabric layer and the test was also applied to the 3-laminated samples in order not to ignore the energy that is not transferred to the test samples. Therefore, the rest of the study was carried out with 3-laminated samples for comparison.

Figure 3. Free fall mechanical tester (a: device overall structure, b: load chamber).

2.2.4 Tensile Tests

In accordance with ASTM D3039 standards, steel plates were adhered to the tensile test specimens with epoxy-based adhesive to prevent the specimens from slipping from the jaws of the test device. The surfaces of the steel plates were sanded with 180 grit sandpaper to ensure better adhesion of the specimens to the jaws. Tensile tests were performed on a 250kN SHIMADZU AG-XPLUS universal tester at a constant speed of 2mm/min. Maximum tensile strength (σ_t) and tensile Young's Modulus (E), were obtained from tensile test data. σ_t is calculated as the ratio between the maximum load achieved during the test and the cross-sectional area. E is calculated considering the linear part of the stress-strain curve.

Table 2. The weights of the core and test samples.

Test	Number of laminates	Label	Weight of core (g.)	Weight of finished part (g.)	Mean weight of finished part (g.)	Weight change of finished part (%)
Tensile	3	3T#1	6.09	13.41	12.87	111.22
	3	3T#2	6.09	13.50		
	3	3T#3	6.10	11.70		
Three-point bending	3	3B#1	5.54	10.60	9.85	78.48
	3	3B#2	5.52	9.42		
	3	3B#3	5.50	9.54		
Drop weight impact	2	2D#1	17.52	32.62	31.53	79.91
	2	2D#2	17.55	31.49		
	2	2D#3	17.52	30.49		
Drop weight impact	3	3D#1	17.53	36.05	35.92	105.14
	3	3D#2	17.50	35.96		
	3	3D#3	17.49	35.74		

2.2.5 Three-point bending tests

Three-point bending tests were performed on the SHIMADZU AGS-X universal tester. The three-point bending test specimen was placed on two supports with a span distance of 80 mm. As seen in Figure 4, the test load was applied from above to the midpoint of the test specimen with a third support at a speed of 10 mm/min. The bending stress (σ_f), strain (ϵ) and elasticity modulus of bending (E_f) were calculated according to the classical beam theory with the data obtained from the three-point bending test. The bending stress is calculated according to equation 1:

$$\sigma_f = \frac{3PL}{2bd^2} \quad (1)$$

where P is the load at which the damage occurs, L is the distance between the support points, b is the sample width, d is the sample thickness. Strain ϵ; is calculated according to equation 2:

$$\epsilon = \frac{6\delta d}{L^2} \quad (2)$$

where δ is the strain of the beam. Flexural modulus of elasticity E_f is calculated according to equation 3:

$$E_f = \frac{L^3 m}{4bd^3} \quad (3)$$

where m is the slope of the load-displacement curve in the linear region.

Figure 4. Three point bending test setup.

3. RESULTS AND DISCUSSION

3.1 Weight and composition of samples

3 number of tensile test specimens with 3-laminated composite, 3 number of three-point bending test specimens with 3-laminated composite, 3 number of drop weight impact test specimens with 2-laminated composite and 3 number of drop weight impact test specimens with 3-laminated composite were produced and labelled. The weights of the core and finished parts obtained as composites are shared in Table 2. The application of carbon fiber reinforced epoxy matrix composite on the PLA core resulted in a significant weight increase relative to the initial core weight. The percentage of weight change between cores and finished parts of the the tensile, three-point bending and drop weight impact test specimens is independent of the initial weight of the specimens. The increase in the number of laminates caused a significant increase in the mean weight of the weight drop test specimens with the same geometry, in which two and three laminates of composite were applied.

Ratio of the fiber reinforcement of laminates was calculated by the ratio of the weight of carbon fiber used to obtain the laminate to the weight of the laminate after curing. Weight carbon fiber was calculated by the difference between the weight of the carbon fiber wrapped core and weight of single core. Weight of the laminate was calculated by the difference between the weight of the finished total part and weight of single core. The calculated fiber reinforcement ratios of the laminates are shared in the Table 3. Composite carbon composition does not differ significantly according to sample geometry or number of laminates.

Table 3. The carbon fiber reinforcement ratio of laminates.

Test	Label	Ratio of the fiber	Mean
Drop weight impact	2D#1	0.47	0.50
	2D#2	0.52	
	2D#3	0.52	
Drop weight impact	3D#1	0.47	0.48
	3D#2	0.47	
	3D#3	0.50	
Tensile	3T#1	0.46	0.53
	3T#2	0.51	
	3T#3	0.62	
Three-point bending	3B#1	0.49	0.55
	3B#2	0.58	
	3B#3	0.57	

3.2 Drop Weight Impact Test Results

The drop weight impact test provides data on the force and displacement on the tip of an impactor when it hits the sample. The resulting force and displacement data provide information such as reaction force, energy, and time to critical damage. The force is zero until the impact tip hits the sample. The occurred force is measured at the time of impact and impact forces continue until the tip stops. The critical force is the initiating force that deals permanent damage. In other words, the first damage in the sample starts to occur at critical force. Then the force reaches its maximum, after which an oscillation is observed up to a second peak force. Critical force must be exceeded for irreversible and visible damage. Otherwise, invisible damage may be observed.
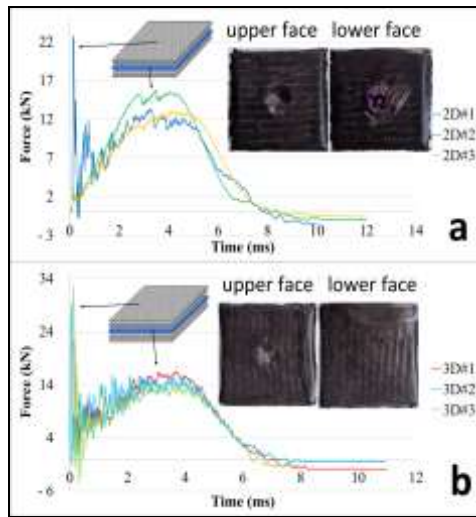
Figure 5. Force-Time curves of a) 2-laminated specimens b) 3-laminated specimens for drop weight impact tests.

For all the samples, an instant force was observed at very initial time of the test and a second force lasting for about 6 seconds occurred (Figure 5). This means that there are two different response type of the sample. The first instant and high force is ascribed to the fabric thermoset layer of the composite, while the second force to thermoplastic core as depicted in Figure 5 inset. This pattern is thought to be characteristic behavior of the composite structure.

In the force-time curve of the 2D#1 sample shown in Figure 5(a), less contact force was observed after the first impact force. In the force-time curves of 2D#2 and 2D#3 samples, the force reached its maximum after the critical impact force. In the force-time curves of all 3-laminated samples as seen in Figure 5(b), less contact force was observed after the first peak force.

The pictures of the tested samples were given in Figure 5. It is clearly seen that the tip penetrated deeply and caused complete damage to the 2-laminated samples. So, the tip did not transfer its energy completely to the test sample, and some energy was absorbed by the lower platform of the instrument. In the case of 3-laminated samples partial damage occurred, and the whole energy was absorbed by the composite sample. From these results, 3 laminate number was determined as critical parameter for drop test. For comperison, only 3-laminated samples were used for the tensile and 3-point bending tests.

While some of the energy of the impactor is absorbed by the sample, some is transferred to the impactor by the elastic restoration of the sample. It can be concluded that the sample exhibits elastic properties as a result of the energy being transmitted back to the impactor rather than being absorbed. The absorbed energy is calculated as the difference between the maximum energy of the impact load and the energy value at which the energy curve begins to stabilize at a plateu. The energy-time curves in Figure 6 show that the impact tip does not fully penetrate the samples and bounces after impact.
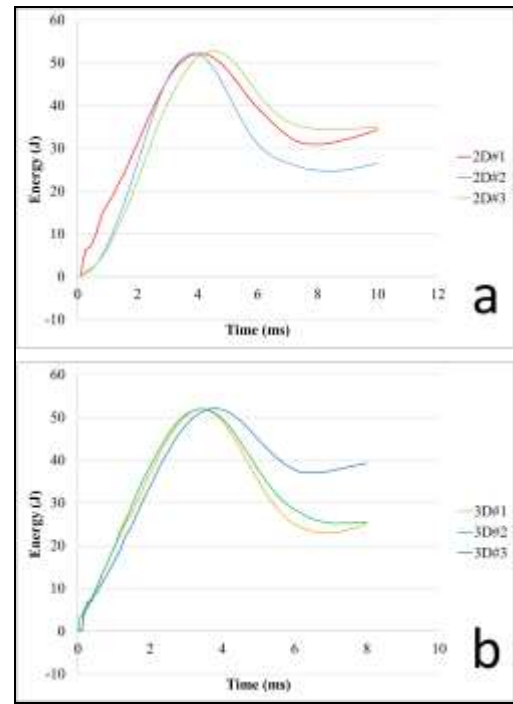

Figure 6. Energy-Time curves of a) 2-laminated specimens b) 3-laminated specimens for drop weight impact tests.

First peak force, second peak force, time to reach to second peak and absorbed energy values obtained from the force-time and the energy-time curves are shown in Table 4. Mean first peak force value of the two laminated is 12.188 kN and three laminated is 28.100 kN. The increase in the first peak force along with the increase in the number of laminates in which the core is wrapped shows that the first peak force is related to the lamina. In addition, the absence of a significant change in the second peak force despite the increase in the number of laminates suggests that the core is effective on the second peak force.

3.3 Tensile Test Results

The stress-strain curves of the tensile test specimens are shown in Figure 7. The samples showed brittle fracture with limited elongation, showing the characteristics of fully composite material. The characteristic of the thermoplastic core was not observed in the stress-strain curves.

Chacon [4] carried out the tensile test with PLA samples produced in the 3D Printer at a fixed loading rate of 2 mm/min. The tensile strengths of the samples with layer thicknesses of 0.18 and 0.24 mm were determined as 76.5 MPa and 73.6 MPa respectively and the modulus of elasticity as 3.882 GPa and 3.915 GPa respectively. In our study, the mean tensile strength (σ_t) of the tensile test specimens is 159.40 MPa and the modulus of elasticity is 2.221 which is shared in Table 5. Comparison of the mechanical properties of the tensile test specimen with the literature shows that the composite laminates applied on the PLA core provide a significant increase in tensile strength.

Table 4. Impact properties of drop weight impact tests specimens.

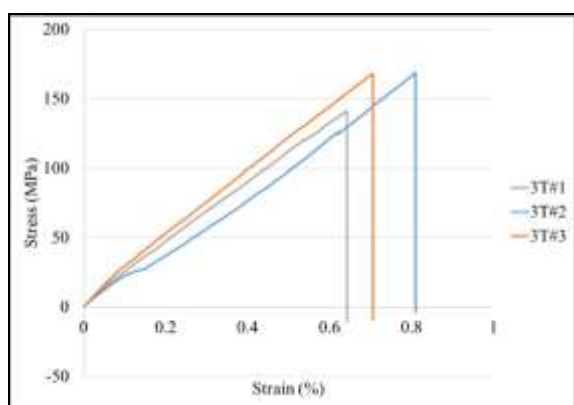| Label	First Peak Force (kN)	Second Peak Force (kN)	Time to reach to second peak (ms)	Absorbed Energy (J)
2D#1	21.469	13.377	3.22	21.20
2D#2	8.277	15.782	3.47	27.50
2D#3	6.819	13.082	4.14	18.21
Mean	12.188	14.080	3.61	22.30
S.D.	8.070	1.481	0.48	4.74
3D#1	22.347	16.532	3.66	29.06
3D#2	29.357	15.897	3.93	26.78
3D#3	32.597	14.373	3.54	15.06
Mean	28.100	15.601	3.71	23.63
S.D.	5.239	1.110	0.20	7.51

Figure 7. Stress-Strain curves of 3-laminated specimens for tensile test.

Table 5. Mechanical strength properties of tensile test specimens.

Label	σ_t (MPa)	Max. Strain	E (GPa)
3T#1	141.22	0.64	2.197
3T#2	168.85	0.81	2.085
3T#3	168.10	0.71	2.382
Mean	159.40	0.72	2.222
S.D.	15.74	0.08	0.150

3.4 Three Point Bending Test Results

Figure 8 shows the bending stress-strain relations of the carbon fiber laminated specimens with 75% infill core. It is clear that the carbon fiber laminates will affect the bending behavior significantly. The bending stress-strain curve exhibits the highest force level to average 138.81 MPa and two enhanced bending stress stages are observed. The first stage of the bending stress is based on the non-elastic characteristic of the CF laminates directly. Elastic properties of the PLA cores support the CF laminates at the second stage of the bending stress.

Chacon [4] carried out the Three-point bending test with PLA samples produced in the 3D Printer at a fixed loading rate of 2 mm/min. The flexural strengths of the samples with layer thicknesses of 0.18 and 0.24 mm were determined as 51.4 MPa and 46.3 MPa respectively and the modulus of elasticity as 1.470 GPa and 1.326 GPa

respectively. In our study, the mean flexural strengths (σ_f) of the tensile test specimens is 138.81 MPa and the modulus of elasticity is 2.001 which is shared in Table 6.
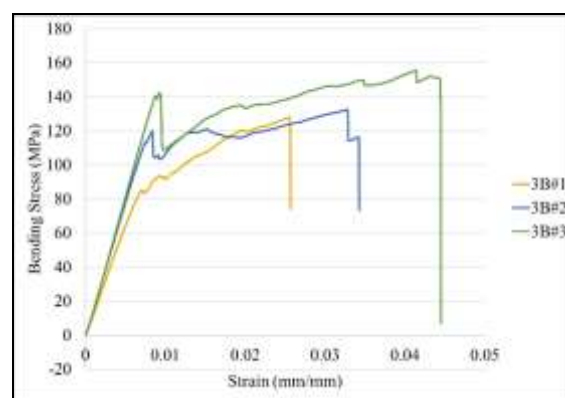

Figure 8. Bending Stress-Strain curves of 3-laminated specimens for three point bending test.

Table 6. Mechanical strength properties of Three-point bending test specimens.

Label	σ_f (MPa)	Max. Strain	E (GPa)
3B#1	128.15	0.03	12.817
3B#2	132.64	0.03	15.743
3B#3	155.64	0.04	16.644
Mean	138.81	0.03	15.068
S.D.	14.75	0.01	2.001

4. CONCLUSION

The tensile and bending test results show that the innovative manufacturing method researched in this study is convenient for the production of 3-dimensional composite objects with complex geometry with no need to molds.

A relation could not be observed between weight of PLA core and finished part when percentage of weight change considered after composite laminates are applied to PLA cores. It is supposed that the most important factor affecting the weight change after the composite laminate is applied is the complexity of the part.

It was observed that while the sample was almost completely damaged in the 2-laminated, the energy was completely absorbed with a slightly damage in the 3-laminated samples. It was determined that the weight of 3-laminated sample increased by 14% compared to 2-laminated sample and First Peak Force of 3-laminated sample was 10% higher. It has been determined that the core with composite laminate exhibits a characteristic behavior.

According to this behavior, it has been determined that the laminate layer absorbs the most of energy in the first phaze, while the core absorbs less energy in the second phase.

Comparison of the mechanical properties of the tensile and three-point bending test specimens with the literature shows that the composite laminates applied on the PLA core provide a significant increase in tensile strength and flexural strength and has a great effect on mechanical properties.

In this study, carbon fiber fabric/epoxy composite samples were prepared by using 75% infill cores produced from PLA with FDM and the effect of number of laminates on mechanical properties was investigated. It is thought that the material used in the production of core and printing parameters of core may have an effect on these properties. It is planned to research these effects in future studies.

Acknowledgement

REFERENCES

1. Guo, N., Leu, M. 2013. Additive manufacturing: technology, applications and research needs. Front. Mech. Eng., 8(3), 215–243.

2. Wong, K. V., Hernandez, A. 2012. A Review of Additive Manufacturing. ISRN Mechanical Engineering, Volume 2012.

3. Parandoush, P., Lin, D. 2017. A review on additive manufacturing of polymer-fiber composites. Composite Structures, 182, 36–53.

4. Chacón, J.M., Caminero, M.A., García-Plaza, E., Núñez, P.J. 2017. Additive manufacturing of PLA structures using fused deposition modelling: Effect of process parameters on mechanical properties and their optimal selection. Materials & Design, 124, 143-157.

5. Melenka, G. W., Cheung, B.K.O., Schofield, J. S., Dawson, M. R., Carey J. P. 2016. Evaluation and prediction of the tensile properties of continuous fiber-reinforced 3D printed structures. Composite Structures, 153, 866–875.

6. Luyt, A.S., Molefi, J.A., Krump, H. 2016. "Thermal, mechanical and electrical properties of copper powder filled low-density and linear low-density polyethylene composites", Polymer Degradation and Stability, 91, 1629-1636.

7. Wang, X., Jiang, M., Zhou, Z., Hui, D. 2017. 3D printing of polymer matrix composites: A review and prospective. Composites, Part B 110, 442-458.

8. Caminero, M.A., Chacón, J.M., García-Moreno, I., Reverte J.M. 2018. "Interlaminar bonding performance of 3D printed continuous fibre reinforced thermoplastic composites using fused deposition modelling", Polymer Testing 68, 415–423.

9. Li, T., Wang, L. 2017. Bending behavior of sandwich composite structures with tunable 3D-printed core materials. Composite Structures, 175, 46–57.

10. Sarvestani H., Akbarzadeh, A.H.,Niknam, H., Hermenean, K. 2018. 3D printed Architected Polymeric Sandwich Panels: Energy Absorption and Structural Performance. Composite Structures, 200, 886-909.

11. Lu C., Qi, M., Islam, S., Chen, P., Gao, S., Xu, Y., Yang, X. 2018. Mechanical Performance of 3D-Printing Plastic Honeycomb Sandwich Structure. Internatıonal Journal Of Precısıon Engıneerıng And Manufacturıng-Green Technology, 5/1, 47-54.

12. Kazmi, S. M. R., Schuster, J., Lutz, J. 2020. Exploring the potential to uniquely manufacture curved VARTM epoxy composites using cost-effective FDM molds. Open Journal of Composite Materials, 10, 45-65.

13. Dippenaar, D.J., Schreve, K. 2013. 3D printed tooling for vacuum-assisted resin transfer moulding. Int. J. Adv. Manuf. Technol., 64, 755–767.

14. Mishra, S., Katti, P., Kumar, S., Bose, S. 2019. Macroporous epoxy-carbon fiber structures with a sacrificial 3D printed polymeric mesh suppresses electromagnetic radiation. Chemical Engineering Journal, 357, 384–394.

15. Besic, E., Valentincic, J., Lebar, A., Jerman, M., Dresar, P., Prijatelj, M., Sabotin, I. 2019. "Composite material manufacturing by 3D Printing and vacuum resin infusion", 17. Research and Science Today, Ek 1/2019, 8-15.